Environmental Science & Technology

pubs.acs.org/est

Article

Monomethylmercury Isotopes Reveal a Hidden Biomagnification Pathway in Marine Ecosystems and Their Environmental Implications

Shaochen Yang, Xingyu Liang, Sae Yun Kwon, Ruolan Li, Chuyan Lai, Martin Tsz-Ki Tsui, David Point, Jinling Liu, Yanxu Zhang, Huan Zhong, Runsheng Yin, Zhengcheng Song, Tian Lin, Jingqian Xie, Li Zhang, Xianzhi Lin, Leiming Zhang, Ping Li,* and Xinbin Feng

Cite This: *Environ. Sci. Technol.* 2026, 60, 5711−5723

Read Online

ACCESS | Metrics & More | Article Recommendations | Supporting Information

ABSTRACT: Monomethylmercury (MMHg) is a potent neurotoxin to which humans are exposed via fish consumption. However, the relative importance of planktonic and benthic biomagnification pathways to fish MMHg concentrations in marine food webs is challenging to quantify. Here, we apply compound-specific isotope analysis (CSIA) of Hg to identify fish MMHg biomagnification pathways across nearshore bay (NB), marine continental shelf (MCS), and pelagic ocean (PO) regions. We observe significant differences in Δ^{199}Hg between MMHg and total mercury (THg), highlighting the limitations of using THg isotopes to resolve MMHg dynamics in the environment. In NB fish, Δ^{199}Hg of MMHg closely matches that of benthic invertebrates, while in MCS and PO fish, it aligns with phytoplankton. According to the MMHg isotope binary mixing model, about 85% of MMHg in NB fish derives from the benthic biomagnification pathway, whereas over 90% of MMHg in MCS and PO fish originates from seawater-phytoplankton trophic transfer. These findings reveal that the benthic biomagnification pathway in near-shore regions has been underestimated in previous models, leading to potential uncertainties in evaluating marine Hg cycling and human exposure risks. This study highlights the importance of the benthic biomagnification pathway in coastal environments and demonstrates the potential of the CSIA of Hg for investigating MMHg biomagnification pathways in marine food webs, which provides new insights for global Hg pollution management under the Minamata Convention.

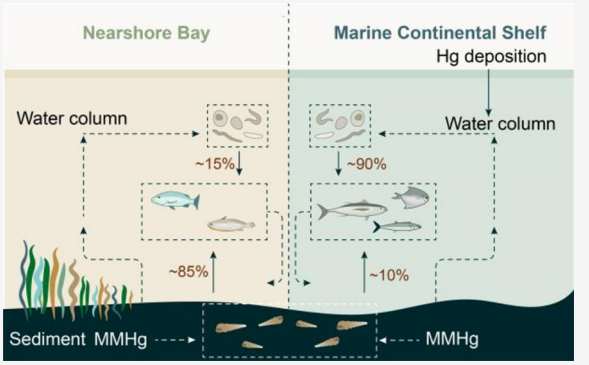

KEYWORDS: *monomethylmercury biomagnification, compound-specific isotope analysis of Hg, marine food web, phytoplankton, benthic invertebrates*

INTRODUCTION

Seafood provides essential nutrients for billions of people worldwide, yet its consumption remains one of the primary routes by which humans are exposed to monomethylmercury (MMHg), a neurotoxic form of mercury (Hg).[1,2] MMHg exposure can cause long-term cognitive and intelligence quotient (IQ) impairments in children.[3] Recent estimates indicate that global socioeconomic costs associated with human MMHg exposure were US$ 117 billion (2020 US$, adjusted by purchasing power parity).[4] With growing global fishery production and trade, per capita seafood consumption has risen from 9.9 kg in the 1960 to over 20 kg by 2020.[5] To address the global health and socioeconomic effects caused by Hg pollution, the Minamata Convention on Mercury—a legally binding international treaty—was adopted in August 2017.[6] A key objective of the convention is to reduce MMHg levels in marine fish via control of anthropogenic Hg emissions.[6,7] Achieving this goal would require a comprehensive understanding of the mechanism of MMHg biomagnification in marine environments.

In marine ecosystems, MMHg is primarily produced in two regions: coastal sediments and the water column of the ocean.[8,9] In pelagic ocean ecosystems, MMHg enters the food web through phytoplankton, which can bioconcentrate MMHg from seawater by factors of 10^4−10^5 times.[10,11] This uptake contributes to significant biomagnification through trophic transfer to zooplankton and high trophic level consumers within a food web that may also involve particle transport or carrion descent processes. In contrast, coastal ecosystems such

Received: September 3, 2025
Revised: January 30, 2026
Accepted: January 30, 2026
Published: February 9, 2026

https://doi.org/10.1021/acs.est.5c12329
Environ. Sci. Technol. 2026, 60, 5711−5723

as nearshore and marine continental shelf regions may biomagnify MMHg via both planktonic and benthic pathways.[12−14] Previous studies have tracked the dietary sources of MMHg in coastal fish via MMHg concentrations among seawater, sediments, and marine organisms.[15−17] These efforts generally suggest a dominant pathway in which MMHg enters coastal waters via riverine inputs and sediment diffusion, is bioconcentrated by phytoplankton, and then biomagnified through the planktonic food web to fish.[9,12,15−17] However, nutrient materials from watershed inputs may shift fish feeding preferences from planktonic to benthic prey, thereby altering their bioaccumulation routes for pollutants.[18] Benthic invertebrates may also assimilate MMHg directly from sediments and porewaters or through the deposition of epipelagic-derived MMHg, and subsequently transfer it to marine fish. The complex hydrodynamic conditions characteristic of coastal ecosystems can also enhance the coupling between planktonic and benthic food chains. The combined influence of these processes makes it difficult to constrain whether MMHg biomagnification in fish is predominantly controlled by planktonic or benthic pathways in coastal ecosystems. This knowledge gap arises from the limitations of concentration-based approaches that cannot adequately account for ecological complexity and multiple interacting drivers. For example, shifts in the composition of dissolved organic matter (DOM) in the water column and organic matter (OM) in sediments may affect the bioavailability and trophic transfer efficiency of MMHg in marine food webs.[11,17] Thus, using Hg concentrations alone to quantify the relative contribution of benthic and planktonic pathways to MMHg biomagnification is insufficient. Due to terrestrial Hg inputs increasingly affecting coastal ecosystems, overlooking the benthic biomagnification pathway may introduce uncertainties into the marine MMHg biomagnification model and MMHg-related health impacts estimation under the implementation of the Minamata Convention.[7,12]

The multidimensional stable isotope system of Hg, including mass-dependent fractionation (MDF; δ^{202}Hg), odd mass-independent fractionation (odd-MIF; Δ^{199}Hg and Δ^{201}Hg), and even mass-independent fractionation (even-MIF; Δ^{200}Hg and Δ^{204}Hg), has proven to be an invaluable tool for distinguishing Hg sources and transformation processes within marine ecosystems.[19−24] MDF occurs during most of the Hg biogeochemical processes, whereas significant odd-MIF is primarily associated with photochemical reactions.[19−21] Given the absence of MIF during trophic transfer,[25,26] the MIF signatures of fish can be used to identify the environmental source of MMHg.[27−30] However, because total Hg (THg) comprises both MMHg and inorganic Hg (IHg), and IHg dominates the Hg pool in phytoplankton and benthic invertebrates, THg measurements cannot reliably resolve the isotopic signature of the MMHg fraction in these organisms.[26,29,31] Thus, understanding MMHg biomagnification pathways remains a certain challenge in the application of THg isotopes to marine food webs. Recently, compound-specific isotope analysis (CSIA) has emerged as an advanced tool to trace environmental pollutants.[32] We expect that MMHg-CSIA can remove the interference from coexisting IHg and enable direct tracking of MMHg transfer through food webs, providing a new tool to address this knowledge gap.[32−34]

In this study, we select three typical marine compartments in China covering nearshore, marine continental shelf, and pelagic ocean regions and measured THg and MMHg-specific isotopes in phytoplankton and benthic invertebrates and THg isotopes in surface seawater, sediment, epipelagic fish (lived in the mid-to-upper water layer), and benthic fish. Through an in-depth analysis of the Hg isotope data, we evaluate the relative contributions of planktonic and benthic pathways to MMHg accumulation in fish across different marine food webs. This work aims to elucidate MMHg biomagnification pathways across different marine compartments and enhance the accuracy of predictions of human MMHg exposure risks in the future, including estimates of associated IQ impacts and socioeconomic costs.

METHODS

Sample Collection and Preparation

A total of 11 seawater, 16 surface sediment and 177 marine biota samples were collected around Daya Bay (nearshore bay food web, hereafter "NB", with water depth <10 m), Zhoushan Island (marine continental shelf food web, hereafter "MCS", with water depth from 20 to 50 m), and the pelagic region of the South China Sea (pelagic ocean food web, hereafter "PO", with water depth >100 m) of China (as shown in Figure S1). Seawater samples were collected from the surface of seawater (0−50 cm depth) by an organic glass water sampler (5L, Loikaw, China). At each seawater sampling site, about 200 mL of seawater samples were filtered with a 0.45 μm filter membrane, acidified with 0.4 mL of HNO_3 (ultrapure, 65%, v/v), and stored in acid-washed Teflon bottles at 4 °C for subsequent THg concentration analysis.[21,35] In addition, approximately 10 L of seawater samples were filtered through a membrane, acidified with 40 mL of ultrapure HNO_3 (65%, v/v), and stored in the dark for Hg isotope analysis.[36] Surface sediment samples were collected from 0−10 cm depth using a customized grab sampler and stored in acid-treated polyethylene bottles at −20 °C in a refrigerator (15 L, Alpicool, China).

Marine organism samples include 21 phytoplankton samples, 26 benthic invertebrate samples, 51 epipelagic fish (living in the mid-to-upper layers of the water column) samples, and 79 benthic fish (living in the bottom layers of the water column) samples. The biological samples were collected in March and September 2023 to reduce potential seasonal variability in solar radiation that could influence MMHg photodegradation and Hg isotope compositions.[10,24] Phytoplankton were collected using a conical phytoplankton net (140 cm in length, with a net opening area of 0.1 m^2 and mesh size of 64 μm) that was horizontally towed at the surface seawater for 4−5 h per site at a speed of 2 nautical miles per hour. After collection, phytoplankton samples were stored in acid-washed polyethylene bottles. Benthic invertebrates (*Turritella terebra sp.*, filter feeders, with the common name of Auger Shell) and marine fish samples were all collected using trawling and sea-fishing expeditions. To minimize the impact of MMHg source mixing caused by fish migration and to ensure that the sampled fish accurately reflect the MMHg isotope characteristics of the local food web,[28,30] we selectively avoided long-distance migratory species according to the fish guidance of China (e.g., tuna, swordfish).[37,38] The Latin name of each collected species is provided in Table S1. The selected fish species exhibit limited short-distance and vertical migration behaviors, thereby aligning more closely with local environmental conditions. As the benthic environment in the PO consists of coral reefs rather than sediment, we have not collected benthic invertebrates for the PO food web. This work collected dorsal muscle tissue of fish and the whole individual of benthic invertebrates for Hg concentration and isotopic analysis. All of the organisms were preserved at −20 °C in the refrigerator prior to analysis. The length, weight, δ^{13}C, and δ^{15}N values of fish and benthic invertebrates were given in Table S1. Details of the δ^{13}C and δ^{15}N measurements are provided in Section S1.

THg and MMHg Concentration Analysis

THg concentrations for seawater (expressed as ng·L^{-1}), sediment (expressed as ng·g^{-1}, dry weight), and marine organism (expressed as

https://doi.org/10.1021/acs.est.5c12329
Environ. Sci. Technol. 2026, 60, 5711−5723

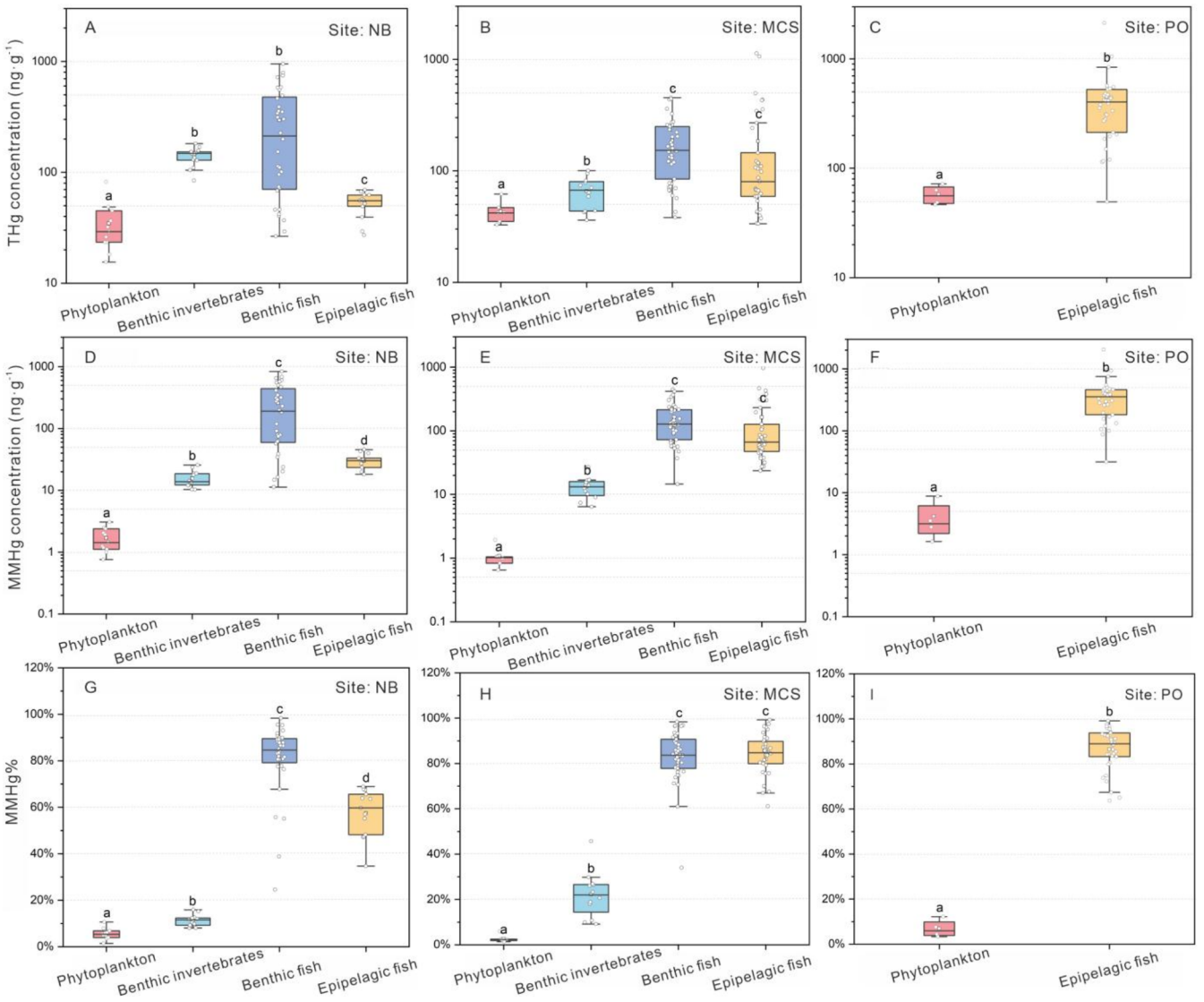

Figure 1. Boxplots of THg (A–C), MMHg (D–F) concentrations, and MMHg% (G–I) in phytoplankton, benthic invertebrates, benthic fish, and epipelagic fish collected from nearshore bay (NB), marine continental shelf (MCS), and pelagic ocean (PO) regions. White solid circles indicate the values of individual samples. Different letters above bars denote statistically significant differences among groups within each site (Mann–Whitney U test, $p < 0.05$).

ng·g^{-1}, dry weight) samples were determined using Brooks Rand Model III cold vapor atomic fluorescence spectroscopy (CVAFS). Seawater samples were pretreated through BrCl oxidation, $SnCl_2$ reduction, and dual amalgamation prior to THg concentration analysis.[35,39] Sediment (about 0.5–1.0 g) and marine organisms (about 0.2–0.5 g) samples were digested with 5 mL of HNO_3 (65%, v/v) and 5 mL of aqua regia at 95 °C for 3 h, respectively.[33,40] The detection limits of THg in water and solid samples were 0.1 ng·L^{-1} and 0.3 ng·g^{-1}, respectively. For the analysis of the MMHg concentrations (expressed as ng·g^{-1}, dry weight), the aquatic organism samples were digested with 25% HNO_3, then measured through aqueous ethylation, purge, trap, and gas chromatography-cold vapor atomic fluorescence spectrometry (GC–CVAFS).[33] The recoveries (%) of THg and MMHg concentrations in certified reference materials (CRMs) ranged from 85 to 110%, ensuring the accuracy of the THg and MMHg analysis.

THg and MMHg Isotope Analysis

THg and MMHg isotopes in the samples were measured by a multicollector inductively coupled plasma mass spectrometer (MC-ICP-MS; Thermo Fisher, Neptune plus, Germany). The THg isotopes for seawater samples were analyzed using the method proposed by Li et al. (2019), while marine organism and sediment samples were analyzed following previous methods based on HNO_3 digestion and aqua regia digestion, respectively.[36,39] The recovery of THg digestion of samples ranged from 85 to 110%, ensuring negligible Hg loss during the isotope pretreatment and analysis.[21] The National Institute of Standards and Technology standard reference materials 3133 (NIST SRM 3133) were spiked to deionized water and determined as CRM (n = 3) for THg isotope analysis in seawater.[21] TORT–3 (Lobster, Canada), BCR–482 (Lichen, Europe), and CC–580 (Sediment, Europe) were used as CRMs of THg isotope analysis. The NIST RM 8610 was used to certify the stabilization of the instrument. Details of THg isotope data for CRMs are given in Table S2.

MMHg isotopes for marine organisms were determined by a selective extraction method (SEM) established by Masbou et al. (2013), which is used for biological samples with low lipid contents.[32] The SEM details are shown in Section S2. The purity and recovery of each sample were determined in order to verify the quality control of MMHg extraction processes.[32,33] The purity is used to evaluate the relative values of the IHg impurities, and the recovery is used to determine the extraction efficiency of MMHg. The mean values of the purity and recovery of samples are 96.1 ± 11.5% and 96.1 ± 12.6%,

https://doi.org/10.1021/acs.est.5c12329
Environ. Sci. Technol. 2026, 60, 5711–5723

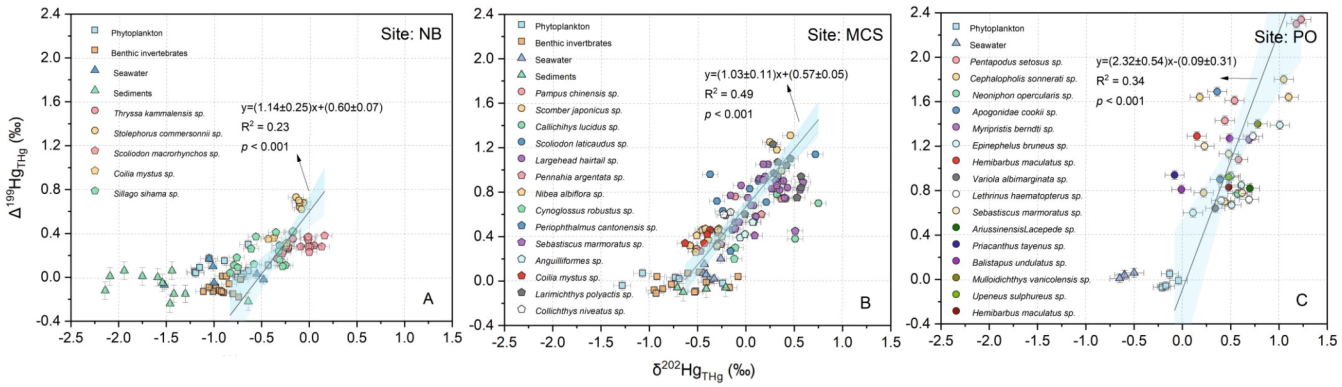

Figure 2. $\delta^{202}Hg_{THg}$ and $\Delta^{199}Hg_{THg}$ values in seawater, sediment, and different marine species samples from nearshore bay (NB; A), marine continental shelf (MCS; B), and pelagic ocean (PO; C) regions. Linear regressions are shown for fish samples, with shaded areas indicating 95% confidence intervals. The SD values of $\delta^{202}Hg_{THg}$ and $\Delta^{199}Hg_{THg}$ for each sample correspond to the analytical uncertainty determined from the matrix-matched certified reference materials. PO fish and seawater isotope data are from Yang et al.[21]

respectively, confirming negligible IHg pollution and Hg loss during the isotope analysis.[32] BCR−414 (Phytoplankton, Europe) and DOLT−5 (Dogfish liver, Canada) were used as CRMs for MMHg isotope analysis of phytoplankton and benthic invertebrate samples, respectively. MMHg isotopes for CRMs determined in this study are given in Table S2.

Quantifying the MMHg Biomagnification Pathway of NB and MCS Fish

Considering that NB and MCS fish primarily accumulate MMHg from both phytoplankton and benthic invertebrates, the biomagnification pathway of MMHg in epipelagic and benthic fish can be estimated using an isotope binary mixing model through Monte Carlo simulations (n = 10,000) with pseudorandom number generation. This approach allows for a thorough evaluation of the effects of error propagation in the binary mixing model calculations.[21] The MMHg contribution (%) of benthic invertebrates (f_{ben}) and phytoplankton (f_{phy}) is calculated as follows

$$\Delta^{199}Hg_{fish} = \Delta^{199}Hg_{MMHg\text{-}ben} \times f_{ben} + \Delta^{199}Hg_{MMHg\text{-}phy} \times f_{ben} \quad (1)$$

$$f_{ben} + f_{phy} = 1 \quad (2)$$

where $\Delta^{199}Hg_{fish}$ represents the $\Delta^{199}Hg$ values of MMHg in epipelagic or benthic fish of NB and MCS (using $\Delta^{199}Hg_{THg}$ to represent MMHg isotope due to the high MMHg% in fish samples). In this study, isotopic data from previous research for NB and MCS fish were incorporated into the model.[21,33,41] $\Delta^{199}Hg_{MMHg\text{-}ben}$ represents the $\Delta^{199}Hg_{MMHg}$ value of benthic invertebrates, while $\Delta^{199}Hg_{MMHg\text{-}phy}$ means the $\Delta^{199}Hg_{MMHg}$ value of phytoplankton. The observation data in this study were modeled via the Gaussian Kernel Density Estimation (GKDE) method. For each Monte Carlo simulation, the mean of 10 randomly selected samples in GKDE (the data fall within the 95% confidence interval) was used as a single observation. Details of the Monte Carlo simulation code are given in Section S3. The probability density of the simulations is provided in Figure S2, and the simulations were conducted via Python 3.9.

Statistical Description

Correlations between measured variables were characterized using linear regression analysis, and the statistical significance of the correlation was calculated by SPSS 19.0 statistical software. All of the averages are expressed as mean ± 1SD. Statistical differences of measured variables are compared using a nonparametric test (Mann−Whitney test) at the 5% significance level. York regression is used for modeling the $\Delta^{199}Hg/\Delta^{201}Hg$ slope. For parameters with defined uncertainty ranges, we perform Monte Carlo simulations (n = 10,000) by randomly sampling values within their respective ranges. This approach allows us to propagate parameter uncertainties through the model and quantify the resulting variability in predicted outcomes.

RESULTS AND DISCUSSION

Hg Concentration in Seawater, Sediment, and Organisms

THg concentrations in surface seawater and sediment are presented in Table S3. Average THg concentrations in seawater are highest in the NB region (2.58 ± 2.46 ng·L^{-1}), followed by the MCS (1.45 ± 0.48 ng·L^{-1}) and PO (1.27 ± 0.40 ng·L^{-1}) regions. These values are comparable (Mann−Whitney test, $p > 0.05$) to those reported for seawater THg concentration in Chinese coastal seas, yet are significantly ($p < 0.05$) higher than those reported for oceanic seawater in the Mediterranean Sea.[21,23] Sediment THg concentrations are comparable between NB and MCS (50.4 ± 18.1 and 49.1 ± 15.6 ng·g^{-1}, respectively, dry weight, $p > 0.05$), which are consistent with those reported for sediments in the Chinese marginal seas.[40]

THg and MMHg concentrations in biota are shown in Figure 1 and Table S4. All of the THg and MMHg concentrations are presented as dry weight in this study. In fish, THg and MMHg concentrations spanned 2 orders of magnitude (from 26.5 to 2130 ng·g^{-1} and from 11.3 to 2040 ng·g^{-1}, respectively). Fish from NB and MCS exhibit comparable THg (224 ± 248 and 186 ± 189 ng·g^{-1}) and MMHg (191 ± 227 and 159 ± 175 ng·g^{-1}) concentrations, which are significantly lower than those in PO fish (451 ± 378 and 403 ± 362 ng·g^{-1}). In addition, both THg and MMHg concentrations are consistently higher in benthic fish than in epipelagic fish (Figure 1A,1B). The fraction of THg present as MMHg (MMHg%) in all sampled fish averages at 81.3 ± 13.4%. All of the phytoplankton and benthic invertebrates samples exhibit relatively low THg (15.1−82.1 and 36.2−181 ng·g^{-1}, respectively) and MMHg (0.651−8.80 and 6.42−26.9 ng·g^{-1}) concentrations compared to fish. THg and MMHg concentrations of phytoplankton and benthic invertebrates in different regions are shown in Figure 1. The MMHg% of phytoplankton (5.00 ± 2.90%) and benthic invertebrates (15.8 ± 9.12%) are significantly lower ($p < 0.05$) than those of fish. In addition, $\delta^{13}C$ and $\delta^{15}N$ values for all biological samples are provided in Table S1. These data offer an essential ecological context for future assessments of trophic structure. However, because the primary objective of this study is to resolve the MMHg biomagnification pathway using Hg isotope signatures

https://doi.org/10.1021/acs.est.5c12329
Environ. Sci. Technol. 2026, 60, 5711−5723

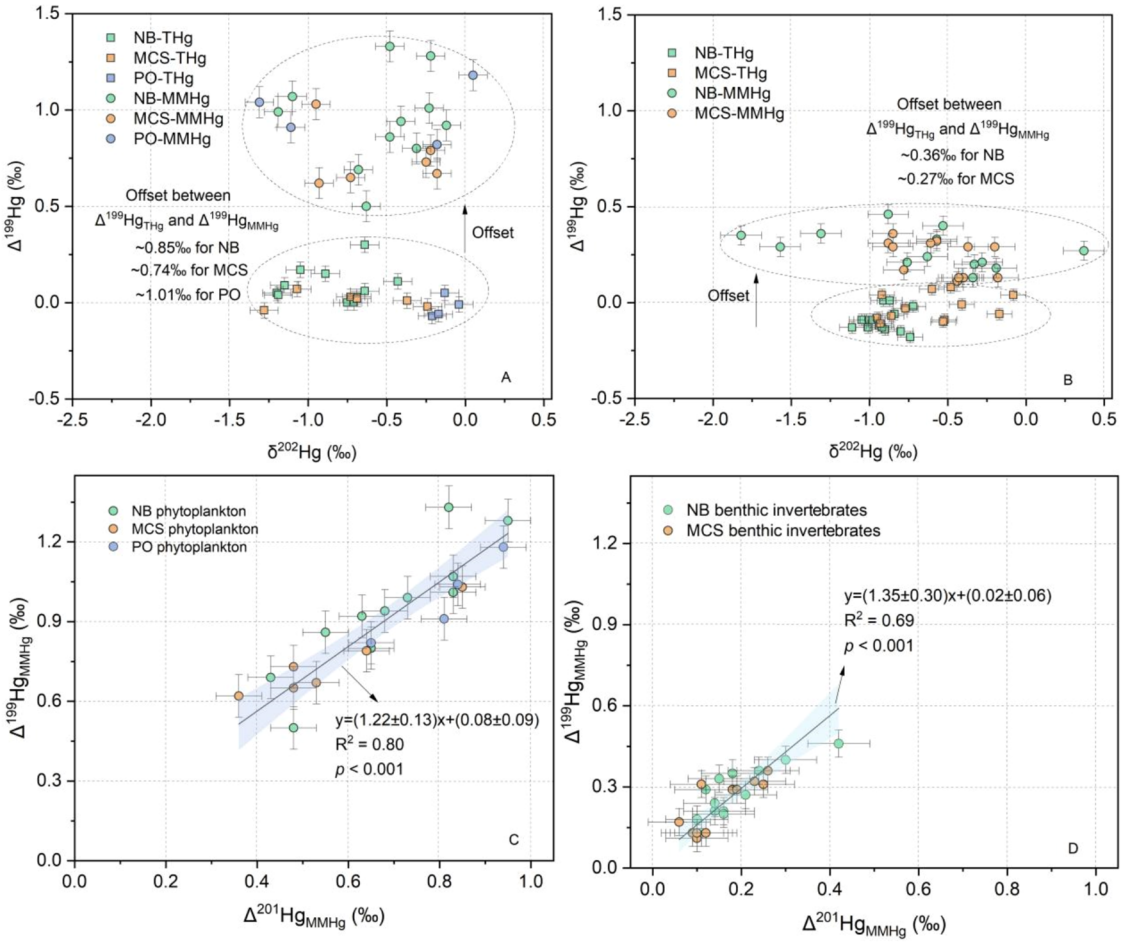

Figure 3. Isotopic characteristics of MMHg and THg in phytoplankton and benthic invertebrates from nearshore bay (NB), marine continental shelf (MCS), and pelagic ocean (PO). (A, B) Comparison of δ^{202}Hg and Δ^{199}Hg between MMHg and THg in phytoplankton (A) and benthic invertebrates (B). The values of Δ^{199}Hg offsets between MMHg and THg of NB, MCS, and PO regions are given in A and B. (C, D) Linear correlations between Δ^{199}Hg and Δ^{201}Hg of MMHg in phytoplankton (C) and benthic invertebrates (D), with shaded areas representing 95% confidence intervals. The analytical SD of isotopic characteristics for each sample corresponds to the analytical uncertainty determined from the matrix-matched certified reference materials.

rather than to quantify trophic magnification factors, we did not further discuss the C and N isotope results here.

THg and MMHg Isotope Compositions in Seawater, Sediment, and Organisms

Values of $\delta^{202}Hg_{THg}$ and $\Delta^{199}Hg_{THg}$ in seawater, sediment, and biota samples are shown in Figure 2. Seawater from NB and MCS regions exhibits distinctively negative $\delta^{202}Hg_{THg}$ values (−0.94 ± 0.38‰ and − 0.37 ± 0.07‰, respectively), along with near-zero $\Delta^{199}Hg_{THg}$ values (0.03 ± 0.09‰ and 0.10 ± 0.07‰). Sediment $\delta^{202}Hg_{THg}$ values are lower in NB (−1.55 ± 0.41‰) than those in MCS (−0.49 ± 0.23‰), while $\Delta^{199}Hg_{THg}$ values remain close to zero in both regions (−0.08 ± 0.10‰ and − 0.07 ± 0.02‰).

Fish from NB and MCS exhibit near-zero $\delta^{202}Hg_{THg}$ values (−0.25 ± 0.24‰ and 0.05 ± 0.34‰, respectively) and slightly positive $\Delta^{199}Hg_{THg}$ values (0.32 ± 0.17‰ and 0.67 ± 0.27‰, respectively). In contrast, fish from the PO region display significantly enriched $\delta^{202}Hg_{THg}$ and $\Delta^{199}Hg_{THg}$ values (0.53 ± 0.32‰ and 1.15 ± 0.46‰, respectively). Across all three regions, $\delta^{202}Hg_{THg}$ and $\Delta^{199}Hg_{THg}$ in fish are positively correlated, with regression slopes of 0.34 ± 0.09, 0.56 ± 0.06, and 0.83 ± 0.20 in NB, MCS, and PO, respectively. Phytoplankton and benthic invertebrates generally exhibit negative $\delta^{202}Hg_{THg}$ values (phytoplankton: −0.85 ± 0.26‰ in NB, −0.60 ± 0.29‰ in MCS, −0.14 ± 0.07‰ in PO; benthic invertebrates: −0.92 ± 0.11‰ in NB, −0.73 ± 0.40‰ in MCS), with $\Delta^{199}Hg_{THg}$ values remaining close to zero (Tables S5 and S6). These isotope values align with their respective seawater and sediment baselines but are substantially lower than those observed in fish (Figure 2). Additional THg isotope data, including $\Delta^{200}Hg_{THg}$ and $\Delta^{201}Hg_{THg}$, are provided in Tables S5 and S6.

$\delta^{202}Hg_{MMHg}$ and $\Delta^{199}Hg_{MMHg}$ values, along with corresponding $\delta^{202}Hg_{THg}$ and $\Delta^{199}Hg_{THg}$ data for phytoplankton and benthic invertebrates from NB, MCS, and PO, are presented in Figure 3A,3B. Other details of MMHg isotope data, including $\Delta^{200}Hg_{MMHg}$ and $\Delta^{201}Hg_{MMHg}$, are provided in Tables S5 and S7. A key finding is that $\Delta^{199}Hg_{MMHg}$ values are significantly higher ($p < 0.05$) than $\Delta^{199}Hg_{THg}$ values in both phytoplankton and benthic invertebrates across all regions. In phytoplankton, $\Delta^{199}Hg_{MMHg}$ values are 0.94 ± 0.24‰ (NB), 0.75 ± 0.15‰ (MCS), and 0.99 ± 0.16‰ (PO), exceeding the corresponding $\Delta^{199}Hg_{THg}$ values by 0.85‰, 0.74‰, and 1.01‰, respectively (Figure 3A). In benthic invertebrates, $\Delta^{199}Hg_{MMHg}$ values are significantly lower than those in phytoplankton ($p < 0.05$), averaging at 0.27 ± 0.10‰

https://doi.org/10.1021/acs.est.5c12329
Environ. Sci. Technol. 2026, 60, 5711−5723

(NB) and 0.24 ± 0.09‰ (MCS), respectively, yet are still elevated relative to the corresponding $\Delta^{199}Hg_{THg}$ by 0.36‰ and 0.27‰ (Figure 3B). A strong linear correlation was observed between $\Delta^{199}Hg_{MMHg}$ and $\Delta^{201}Hg_{MMHg}$ in both phytoplankton and benthic invertebrates, with nearly identical slopes of 1.28 ± 0.14 and 1.27 ± 0.17, respectively (Figure 3C,D).

In contrast, differences in δ^{202}Hg between MMHg and THg are less consistent. Significant enrichment in $\delta^{202}Hg_{MMHg}$ relative to $\delta^{202}Hg_{THg}$ is observed only in NB phytoplankton (−0.53 ± 0.35‰) and benthic invertebrates (−0.66 ± 0.58‰; $p < 0.05$), while no significant differences are found in MCS (phytoplankton: −0.54 ± 0.37‰; benthic invertebrates: −0.55 ± 0.25‰) or PO (phytoplankton: −0.64 ± 0.67‰; $p > 0.05$). Additionally, comparisons of Δ^{200}Hg between MMHg and THg across all phytoplankton and benthic invertebrate samples show no significant differences (Figure S3).

New Insights into MMHg Dynamics at the Food Web Base

Although numerous studies have demonstrated that MIF is not induced during trophic transfer, previous research studies observed consistently lower $\Delta^{199}Hg_{THg}$ values in benthic invertebrates compared to fish across diverse ecosystems, including marginal seas,[22] estuaries,[27] rivers,[31] and plateau lakes.[42] These patterns, along with linear correlations between $\Delta^{199}Hg_{THg}$ and MMHg% in biota, lead to the hypothesis that such isotopic disparities reflect the differing proportions and isotope compositions of MMHg and IHg, rather than trophic effects alone.[22,27,31,42] The MMHg% in phytoplankton and benthic invertebrates observed in this study are relatively low and exhibited a narrow range in a global context.[19,27] This may reflect the influence of intensive anthropogenic activities and elevated nutrient levels in Chinese coastal waters, which enhance primary production and result in growth dilution effects on MMHg bioaccumulation.[43] Thus, the $\Delta^{199}Hg_{THg}$ values primarily reflect the isotopic signature of IHg, and therefore provide limited insight into the MMHg isotope composition of phytoplankton and benthic invertebrates in this study. Here, we used the MMHg-CSIA method to determine $\Delta^{199}Hg_{MMHg}$ values for both phytoplankton and benthic invertebrates, indicating that $\Delta^{199}Hg_{MMHg}$ is significantly higher than $\Delta^{199}Hg_{THg}$ ($p < 0.05$) within the same organism (Figure 3A,3B), providing direct quantification of the isotopic offset between MMHg and THg. Importantly, this offset differed between phytoplankton and benthic invertebrates; this finding cannot be resolved using THg isotope and MMHg/THg ratio linear correlations alone, suggesting that THg-based isotope data can mask MMHg-specific processes and that CSIA is required to resolve distinct MeHg pathways at the base of marine food webs.

To explain these positive MIF signatures in MMHg, we examined the slopes of $\Delta^{199}Hg_{MMHg}/\Delta^{201}Hg_{MMHg}$. Here, the $\Delta^{199}Hg_{MMHg}/\Delta^{201}Hg_{MMHg}$ ratio in phytoplankton (1.22 ± 0.13) and benthic invertebrates (1.35 ± 0.30) is closely aligned with that in marine fish (1.20 ± 0.01), rather than sediment or seawater (0.88 ± 0.11; Figures 3C,3D and S4). The $\Delta^{199}Hg/\Delta^{201}Hg$ slope can be an efficient proxy to distinguish between MMHg photodegradation, which showed a slope of 1.36 ± 0.04 (1SE) from experimental data, and IHg (normally as aqueous Hg(II)) photoreduction,[41,44] which has a slope of 1.00 ± 0.02.[44,45] Previous observations have reported a $\Delta^{199}Hg/\Delta^{201}Hg$ ratio of 1.20 ± 0.02 for marine fish (Figure S5), which is lower than the value from experimental MMHg photodegradation;[21,44] this can be explained by the compositional differences in DOM or Hg-binding ligands between natural and experimental conditions. Therefore, the positive $\Delta^{199}Hg_{MMHg}$ values of phytoplankton and benthic invertebrates are caused by photodegradation of MMHg, rather than Hg(II) photoreduction, followed by methylation. Different odd-MIF signatures observed in phytoplankton (∼1.00‰) and benthic invertebrates (∼0.30‰) suggest the distinct MMHg photochemical processes.

In phytoplankton, which can assimilate MMHg directly from the dissolved phase, the positive $\Delta^{199}Hg_{MMHg}$ values likely result from the uptake of MMHg that had undergone photodegradation in seawater at the euphotic zone.[46,47] By contrast, benthic invertebrates are generally considered as sediment-dwelling filter feeders, and the accumulated MMHg is typically assumed to originate from in situ methylation of IHg within anoxic sediments, where exposure to sunlight is minimal and photochemical alteration is not expected.[22,27,31,40] A plausible explanation is that photodegraded MMHg produced in surface waters is adsorbed onto sinking particles or particulate organic matter, subsequently transported to surface sediments, and ultimately assimilated by benthic fauna.[9] This vertical transfer mechanism expands current understanding of MMHg cycling and highlights the potential for euphotic photochemical processes to influence the benthic MMHg pool. Given that the Hg methylation process does not cause MIF, the $\Delta^{199}Hg_{THg}$ of sediments can be used to represent the isotopic signature of *in situ* produced MMHg in sediments. In addition, the $\Delta^{199}Hg_{MMHg}$ of phytoplankton can be characterized as the isotopic signature of epipelagic MMHg in seawater. Using these two isotopic end-members and a binary isotope mixing model (Section S4), we quantified the contribution of epipelagic MMHg to the MMHg accumulated in benthic invertebrates. The results indicate that approximately 35.3 ± 15.4% of the MMHg in NB benthic invertebrates and 38.8 ± 14.1% in those from the MCS region originate from photodegraded MMHg exported from the surface seawater. These findings demonstrate an obvious vertical deposition of MMHg across contrasting marine environments and provide quantitative insights for understanding the biogeochemical cycling of MMHg in marine ecosystems.

With the photochemical origin of MMHg odd-MIF established, we further investigate how this isotopic signal reflects the intensity and variability of MMHg photodegradation across coastal-to-oceanic gradients. The absence of odd-MIF during trophic transfer allows $\Delta^{199}Hg_{THg}$ of fish to represent the degrees of MMHg photodegradation in seawater.[21,48] Here, our findings reveal a gradient of $\Delta^{199}Hg_{THg}$ values in fish: PO (1.15 ± 0.46‰) > MCS (0.67 ± 0.28‰) > NB (0.32 ± 0.17‰). However, the odd-MIF signatures of phytoplankton diverge from this trend. The $\Delta^{199}Hg_{MMHg}$ values of NB (0.94 ± 0.24‰) and MCS (0.75 ± 0.15‰) phytoplankton are comparable ($p > 0.05$); while that of PO (0.99 ± 0.16‰) is similar to that of NB ($p > 0.05$), but is significantly higher than that of MCS ($p < 0.05$; Figure 3A). Phytoplankton can directly assimilate MMHg from seawater and therefore reflect the short-term photochemical history of MMHg, whereas fish integrate MMHg isotope signals over longer periods and indicate broader habitat information.[46,47] Despite the variations of seasons and habitat depth may lead to $\Delta^{199}Hg_{MMHg}$ differences between fish and phytoplankton, the differences in the NB region are significantly higher than those

https://doi.org/10.1021/acs.est.5c12329
Environ. Sci. Technol. 2026, 60, 5711−5723

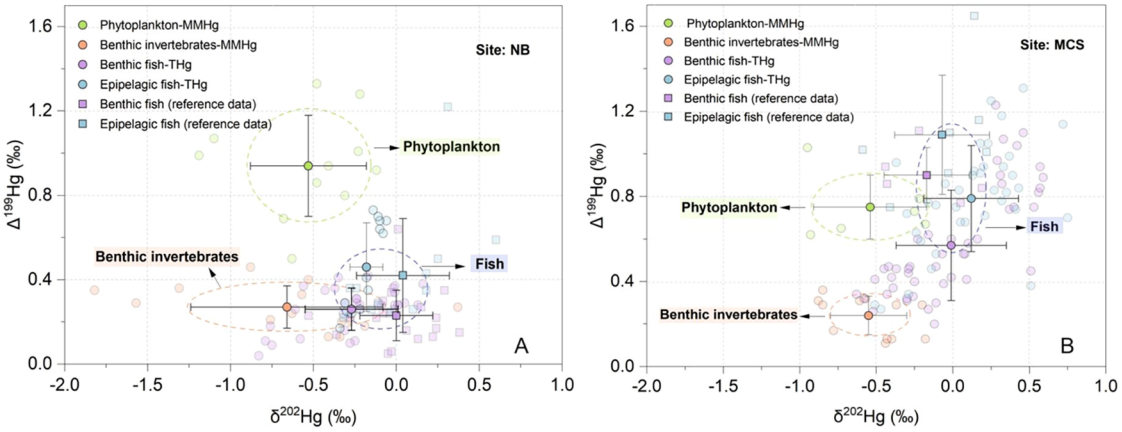

Figure 4. Isotopic composition of MMHg in phytoplankton and benthic invertebrates compared to THg isotopes in marine fish from nearshore bay (NB) (A) and continental shelf (MCS) (B) food webs. Plots show δ^{202}Hg and Δ^{199}Hg values for MMHg in phytoplankton and benthic invertebrates, and for THg in benthic and epipelagic fish. Average (±1SD) values of each group are shown as bold markers with error bars, while individual samples are plotted as pale points. Ellipses highlight the isotopic distribution of phytoplankton, benthic invertebrates, and fish. Reference fish data for NB are from Yin et al.[41] and Yang et al.,[21] and for MCS from Yang et al.[33]

in the MCS and PO regions. This pattern may reflect the complex coupling between benthic and pelagic processes in shallow hydrological ecosystems in the NB region, where benthic-derived MMHg can enter fish and influence their isotopic signatures. The underlying mechanisms are further discussed below.

In addition, previous studies have suggested that increasing light intensity from nearshore to open-ocean environments leads to a gradient of increasing photochemical degradation in seawater.[21,30] However, we do not observe an increase in phytoplankton $\Delta^{199}Hg_{MMHg}$ values from nearshore regions to the PO. The similarity in phytoplankton $\Delta^{199}Hg_{MMHg}$ values between the NB and PO may be attributed to two factors. First, coastal systems such as the NB are characterized by complex and elevated DOM pools, which can enhance photochemical demethylation via DOM-mediated radical pathways, potentially resulting in higher $\Delta^{199}Hg_{MMHg}$ signatures produced in surface waters.[49] Second, in the PO, phytoplankton biomass is more likely concentrated at depth within the deep chlorophyll maximum (DCM), typically below ∼50 m. MMHg associated with phytoplankton in the DCM would experience reduced photodegradation relative to surface waters and may subsequently be transported upward through vertical mixing or upwelling, thereby contributing to lower $\Delta^{199}Hg_{MMHg}$ values observed in surface phytoplankton.[50,51] This process may decrease the $\Delta^{199}Hg_{MMHg}$ values in the PO and MCS regions, thereby reducing the isotopic contrast relative to the NB. This finding provides a basis for understanding MMHg photodegradation and the resulting odd-MIF signatures across coastal-to-oceanic seawater.

Hidden MMHg Biomagnification Revealing by MMHg Isotopes

Based on our compound-specific isotopic data, the linkage of MMHg among marine fish, phytoplankton, and benthic invertebrates can be established as shown in Figure 4. Since MMHg is the predominant form (>80%) in marine fish,[51,52] we use $\Delta^{199}Hg_{THg}$ to represent the MMHg isotopic signature in fish samples.[21] In the NB and MCS regions, the distinct $\Delta^{199}Hg_{MMHg}$ values between phytoplankton and benthic invertebrates allow them to serve as two isotopic end-members to quantify the MMHg biomagnification pathway (Figure 4A). It is worth noting that suspended particulate matter (SPM) may also contribute a fraction of MMHg to marine fish.[19] Because this study focuses on trophic transfer from lower trophic level biota to fish, the SPM is not included as an end-member in the isotope mixing model.

The similar $\Delta^{199}Hg_{THg}$ values between benthic fish (0.26 ± 0.10‰) and benthic invertebrates (0.27 ± 0.10‰; $p > 0.05$) in NB suggest that ∼100% of MMHg in benthic fish originates from benthic invertebrates. This finding is consistent with prior studies reporting that MMHg in sediment can be directly assimilated by benthic invertebrates and subsequently transferred to benthic fish.[12,17] Surprisingly, the $\Delta^{199}Hg_{THg}$ values for epipelagic fish (0.46 ± 0.21‰) are significantly lower than $\Delta^{199}Hg_{MMHg}$ observed in phytoplankton (0.94 ± 0.24‰) in NB, which is consistent with herbivorous fish of previous work conducted in Pearl River Estuary (0.36 ± 0.18‰, $n = 9$).[41] Using a binary mixing model for MMHg isotopes (see Methods section Quantifying MMHg biomagnification pathway of NB and MCS fish), we estimate that only 26.2 ± 13.9% of MMHg in epipelagic fish in NB is derived from phytoplankton, with the remaining fraction originating from the benthic invertebrates. These findings challenge the long-standing assumption that planktonic food web biomagnification dominates MMHg accumulation in nearshore epipelagic fish, highlighting the underestimated role of benthic biomagnification pathways.

Recent ecological studies have shown that anthropogenic nutrient inputs can substantially enhance phytoplankton productivity in nearshore ecosystems (e.g., estuaries within ∼10 km from the coastline).[53,54] However, the increase in primary production is not efficiently transferred to zooplankton through the planktonic food web, as alterations in N:P or Si:P ratios can promote the dominance of larger or chemically defended phytoplankton taxa, which reduce grazing efficiency by zooplankton due to increased cell size, structural defenses, or reduced nutritional quality.[55−57] Instead, deposited organic matter stored in sediments represents a more stable and accessible carbon source for benthic invertebrates (e.g., annelids and gastropods), which subsequently play a key role in transferring energy to epipelagic fish.[57] Thus, MMHg biomagnification in the NB food web is primarily driven by a benthic pathway, where MMHg in the environment is directly

https://doi.org/10.1021/acs.est.5c12329
Environ. Sci. Technol. 2026, 60, 5711−5723

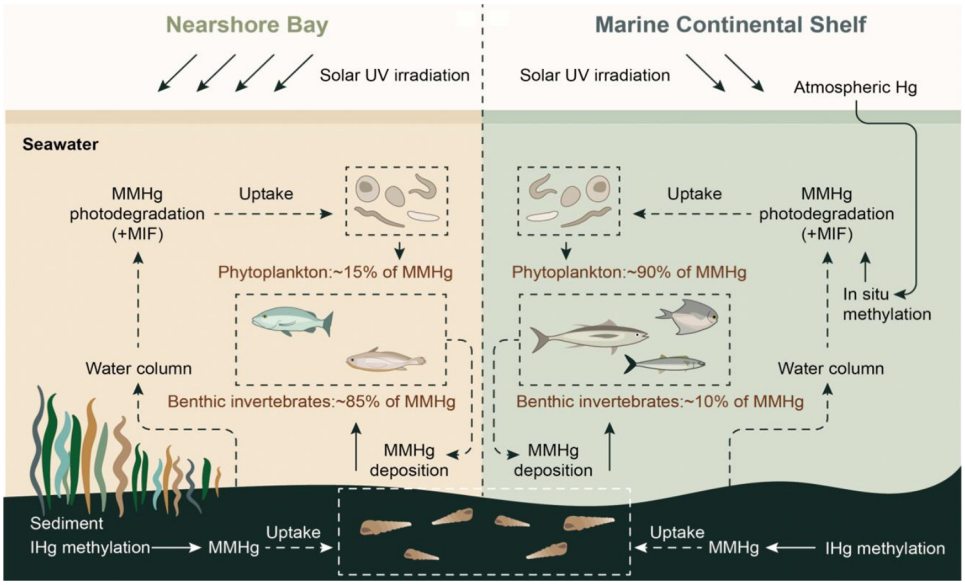

Figure 5. Conceptual model of MMHg biogeochemical pathways in nearshore bay (NB) and marine continental shelf (MCS) ecosystems. This schematic illustrates MMHg production, transformation, and trophic transfer processes across benthic and planktonic compartments. In NB, fish predominantly acquire MMHg from benthic invertebrates (~85%), while phytoplankton contribute only ~15%. In contrast, the MCS food web is dominated by the planktonic pathway, with phytoplankton contributing ~90% of fish MMHg. MMHg photodegradation (marked by Δ^{199}Hg MIF) occurs in surface waters in both ecosystems. Sinking particles mediate vertical MMHg deposition, connecting photochemically modified MMHg to benthic invertebrates. This framework highlights a spatial shift from benthic- to planktonic-dominated MMHg biomagnification within NB and MCS regions.

assimilated by benthic invertebrates. This MMHg is subsequently transferred through trophic interactions to higher trophic-level organisms, including both benthic and epipelagic water-column fish, leading to substantial MMHg biomagnification. These results collectively support the central role of sedimentary MMHg in aggravating near-shore fish contamination through the benthic food web. The consistent Δ^{199}Hg values of MMHg between benthic fish and benthic invertebrates underscore a direct trophic linkage, while the limited phytoplankton-derived MMHg in epipelagic fish highlights the broader reach of sediment-sourced MMHg beyond benthic habitats in nearshore regions. Although previous studies have noted weak statistical correlations between sediment and fish MMHg concentrations,[12,16,17] our findings suggest that such discrepancies may stem from overlooking the mediating role (e.g., bioaccumulation efficiency and feeding behavior) of benthic invertebrates, which act as key conduits between sedimentary MMHg pools and higher trophic levels. Therefore, sediment MMHg concentrations remain a critical predictor of fish contamination in nearshore regions, particularly when considered in conjunction with benthic biomass and food web structure.

Conversely, in the MCS region, $\Delta^{199}Hg_{THg}$ values of epipelagic fish are comparable with $\Delta^{199}Hg_{MMHg}$ of phytoplankton (0.75 ± 0.15‰; $p > 0.05$; Figure 4B), suggesting that ~100% of MMHg in MCS epipelagic fish is derived from phytoplankton consumption. $\Delta^{199}Hg_{THg}$ values of benthic fish (0.57 ± 0.26‰; $p < 0.05$) are significantly lower than those of epipelagic fish, and fall between the $\Delta^{199}Hg_{MMHg}$ of phytoplankton and benthic invertebrates (0.24 ± 0.09‰). The MMHg isotope binary mixing model output shows that phytoplankton contributes 73.1 ± 20.0% of MMHg to the MCS benthic fish. It has been demonstrated that benthic fish in continental shelf regions exhibit lower $\Delta^{199}Hg_{THg}$ values compared to epipelagic fish, primarily due to contributions from the benthic food web.[58] Our study quantifies this contribution, revealing that in the MCS region, the benthic food web accounts for less than 30% of MMHg in benthic fish. Compared to the NB region, the MCS region is less influenced by anthropogenic activities, particularly nutrient inputs, resulting in a relatively stable phytoplankton community, which facilitates phytoplankton to serve as the primary entry point for MMHg. Organic particles and zooplankton grazing on phytoplankton can transfer surface MMHg to benthic fish and constructing a planktonic biomagnification pathway.[12] However, MMHg accumulated in benthic invertebrates shows a limited transfer to higher trophic-level fish within the MCS region.

According to the average yields of benthic and epipelagic fish captured from Chinese coastal waters from 2011 to 2020 (Table S8),[59] a Monte Carlo simulation (Section S5) estimates that phytoplankton contributes only 14.8 ± 9.09% of MMHg to the overall fish (including epipelagic and benthic fish) in the NB region, but as high as 90.1 ± 19.0% in the MCS region. Although sediment is regarded as the dominant source of MMHg for both NB and MCS fish,[8,21,27] the MMHg biomagnification pathways of these two ecosystems are different. Based on the analysis of compound-specific MMHg isotopes presented above, we develop a conceptual model for marine MMHg biogeochemical processes (Figure 5), which reveals that the assimilation of MMHg by benthic invertebrates is the dominant pathway (>85%) of MMHg entering NB food webs, while the uptake of MMHg by phytoplankton is the major pathway (>90%) of MMHg entering MCS food webs. We suggest that benthic invertebrates may act as "carbon supply" within NB food webs, becoming the primary dietary source of MMHg for local fish under scenarios with aggravated human activity effects. In contrast, phytoplankton plays a dominant role in MMHg biomagnification in the MCS region. With decreasing impacts from anthropogenic activities in MCS

https://doi.org/10.1021/acs.est.5c12329
Environ. Sci. Technol. 2026, 60, 5711−5723

than NB, the dominant contributor to MMHg biomagnification shifts from benthic invertebrates to phytoplankton, reflecting changes in the ecological dynamics of the food web. A concentration-based mass-balance model for benthic and pelagic food webs was not applied in this study because uncertainties associated with prey-specific feeding rates and trophic transfer may affect such estimates.

It should be noted that the results presented here are intended to elucidate MMHg biomagnification pathways within marine food webs (i.e., planktonic versus benthic pathways) rather than to distinguish the relative contributions of water column-produced versus sediment-produced MMHg to fish. For highly coupled ecosystems such as the NB, quantitatively identifying environmental sources would require direct MMHg isotope measurements in both the water column and sediments, which will be conducted in future works. Despite this, our results still suggest that the role of benthic food webs in fish MMHg accumulation may have been underestimated in previous studies.

This work also investigates the MMHg biomagnification pathway in the PO region (Figure S6). $\Delta^{199}Hg_{THg}$ values of epipelagic fish (1.15 ± 0.46‰) are comparable ($p > 0.05$) with $\Delta^{199}Hg_{MMHg}$ values of phytoplankton (0.99 ± 0.16‰), suggesting that most MMHg in fish is derived from phytoplankton in PO. Therefore, the planktonic pathway is the major MMHg biomagnification pathway in the PO food web, as is also the case in the MCS food web (Figure 5B). The PO region is not affected by sediment and terrestrial input, leaving atmospheric deposition as the most important Hg source.[21,23] Atmospheric Hg(II) deposited into the water column can be methylated to MMHg,[9,19] then assimilated by phytoplankton, and finally accumulate in the upper PO food web.

Implications of Marine MMHg Contamination

Understanding the contributions of planktonic and benthic pathways to MMHg accumulation in marine fish is essential for predicting seafood-related Hg risks. Although THg isotopes have recently been used as an effective tracer in marine ecosystems,[21,22,24] the significant differences of isotopic values observed between MMHg and THg in phytoplankton and benthic invertebrates show the limitations of THg isotopes in elucidating MMHg biomagnification pathways in the marine food web. Here, our observation presents a conceptual figure of marine MMHg biogeochemical processes based on compound-specific MMHg isotopes (Figure 5), and it reveals that the assimilation of MMHg by benthic invertebrates is the dominant pathway of MMHg entering NB food webs, while the uptake of MMHg by phytoplankton is the major pathway of MMHg entering PO and MCS food webs. This study decoded the quantification of the relative importance of planktonic and benthic food webs to MMHg accumulation in fish across different marine ecosystems. Previous models primarily used the planktonic biomagnification pathway to predict the MMHg concentrations in marine fish under the combined effect of Minamata Convention implementation and climate change.[7,60−62] This pattern is likely applicable to the MCS and PO regions, while it appears to be less relevant to the NB region. Furthermore, the shift of the MMHg biomagnification pathway in NB and MCS suggests that the fish MMHg levels in these two regions may respond differently to reductions in atmospheric Hg. In the NB, fish Hg is largely influenced by the benthic MMHg pool, which responds slowly to changes in external inputs; whereas fish in the MCS primarily reflect the epipelagic MMHg pool, which responds more rapidly to changes in atmospheric Hg deposition. Accordingly, fish Hg concentrations in the MCS are likely to decrease more quickly as the Minamata Convention continues to be implemented. These findings offer new insights for marine MMHg risk prediction under the implementation of the Minamata Convention.

The nearshore region is defined as coastal areas within approximately 10 km of the shoreline,[63] such as estuaries and nearshore bays, which are subject to strong land−sea interactions. Nearshore fisheries contribute over 20% of global seafood and represent a critical protein source for coastal populations.[64,65] Therefore, this study further estimates the global health impact of neglecting benthic MMHg biomagnification processes (Section S6 and Table S9). The results show that fish MMHg concentrations predicted under the benthic pathway are consistently higher than those from the planktonic pathway (Figure S7), which is consistent with prior trophic transfer models by Wu and Zhang (2023).[7] This pattern is largely driven by terrestrial Hg inputs to nearshore zones via riverine discharge.[66] Our simulations also indicate that incorporating the benthic pathway, compared to models considering only the planktonic route, may lead to an aggregate IQ loss of 0.020 to 0.049 points (95% confidence interval) in populations across different countries and an associated annual economic loss of over US$ 19 billion globally (Figure S8). However, the NB site in this study is a shallow (<10 m) environment strongly influenced by terrestrial inputs and anthropogenic activities, and its food web structure may not be fully representative of all of the global nearshore ecosystems. Extrapolating NB-based patterns in this study to less terrestrially influenced nearshore regions may remain uncertainties. Despite these, our estimates aim to illustrate the potential magnitude of bias that may arise when benthic biomagnification pathways are excluded from MMHg exposure assessments. Future work is needed to include observations from a wider range of nearshore regions to clarify how MMHg biomagnification processes shift across nearshore environments that differ in the intensity of terrestrial and anthropogenic effects.

Through the application of MMHg-CSIA to low MMHg% organisms, this study identifies benthic pathways as a previously underestimated mechanism of MMHg biomagnification in nearshore ecosystems. Integrating this pathway into current marine Hg models can enhance the accuracy of marine MMHg contamination predictions. For example, reducing watershed Hg discharge and sediment disturbance may effectively limit the transfer of benthic MMHg to fish. Accounting for this biological biomagnification can help manage future MMHg exposure risks in seafood consumers under changing environmental conditions. We further suggest that the application of MMHg-CSIA to track MMHg biomagnification provides an effective approach for refining marine Hg models and may serve as a valuable tool for assessing MMHg contamination risks in other ecologically vulnerable regions, such as hadal zones or polar marine environments.

https://doi.org/10.1021/acs.est.5c12329
Environ. Sci. Technol. 2026, 60, 5711−5723

■ ASSOCIATED CONTENT

Supporting Information

The Supporting Information is available free of charge at https://pubs.acs.org/doi/10.1021/acs.est.5c12329.

Sections (S1−S6), Tables (S1−S9), and Figures (S1−S8); C and N isotopes measurements (Section S1); details of MMHg isotope analysis (Section S2); Monte Carlo simulation for estimation of the biomagnification pathway (Section S3); vertical MMHg deposition in NB and MCS (Section S4); estimation of overall fish MMHg dietary sources (Section S5); estimation of global IQ and economic loss from the benthic MMHg biomagnification pathway (Section S6); detailed information on sample number, species, length (cm), and weight (g) in marine fish, benthic invertebrates and phytoplankton captured from nearshore bay (NB), marine continental shelf (MCS), and pelagic ocean (PO) regions; (Table S1); quality control (Mean ± 2SD) of THg and MMHg isotope ratios of certified reference materials (Table S2); THg concentrations of seawater and sediment collected from nearshore bay (NB), marine continental shelf (MCS) and pelagic ocean (PO) regions (Table S3); THg and MMHg concentrations as well as the fraction of MMHg in THg (MMHg%) of marine fish, benthic invertebrates and phytoplankton collected in nearshore bay (NB), marine continental shelf (MCS) and pelagic ocean (PO) regions (Table S4); mean (±1SD) values of THg and MMHg isotope compositions of seawater, sediment and marine organisms in this study (Table S5); THg isotope ratios of seawater, sediment, marine fish, benthic invertebrates and phytoplankton collected from nearshore bay (NB), marine continental shelf (MCS) and pelagic ocean (PO) regions (Table S6); MMHg isotopes of benthic invertebrates and phytoplankton collected from nearshore bay (NB), marine continental shelf (MCS) and pelagic ocean (PO) regions (Table S7); summary of marine fish catches in China from 2011 to 2020 (Table S8); coastal seafood production, coastal seawater and sediment Hg concentrations, modeled fish MMHg concentration (mean value), total population, and birth counts in major seafood-producing countries (data are collected from 2021) (Table S9); map of the sampling locations (Figure S1); distribution of Δ^{199}Hg of MMHg simulated by Gaussian Kernel Density Estimation (KDE) in Monte Carlo model (Figure S2); Δ^{200}Hg values of THg and MMHg of phytoplankton and benthic invertebrates samples collected from nearshore bay (NB), marine continental shelf (MCS) and pelagic ocean (PO) food webs (Figure S3); the $\Delta^{199}Hg_{THg}/\Delta^{201}Hg_{THg}$ slope of seawater and sediment collected from nearshore bay (NB), marine continental shelf (MCS) and pelagic ocean (PO) (Figure S4); $\Delta^{199}Hg_{THg}/\Delta^{201}Hg_{THg}$ slope of marine fish collected from nearshore bay (NB), marine continental shelf (MCS), and pelagic ocean (PO) food webs (Figure S5); $\delta^{202}Hg_{MMHg}$ and $\Delta^{199}Hg_{MMHg}$ of phytoplankton and $\delta^{202}Hg_{THg}$ and $\Delta^{199}Hg_{THg}$ of marine fish in pelagic ocean (PO) food webs (Figure S6); simulated fish MMHg concentrations ($ng \cdot g^{-1}$, wet weight) under two biomagnification pathways (benthic and planktonic) across 29 coastal countries (Figure S7); and additional IQ loss and economic impacts induced by the benthic MMHg biomagnification in nearshore fisheries (Figure S8) (PDF)

■ AUTHOR INFORMATION

Corresponding Author

Ping Li − *State Key Laboratory of Environmental Geochemistry, Institute of Geochemistry, Chinese Academy of Sciences, Guiyang 550081, China;* orcid.org/0000-0002-0145-4122; Email: liping@mail.gyig.ac.cn

Authors

Shaochen Yang − *State Key Laboratory of Environmental Geochemistry, Institute of Geochemistry, Chinese Academy of Sciences, Guiyang 550081, China*

Xingyu Liang − *State Key Laboratory of Environmental Geochemistry, Institute of Geochemistry, Chinese Academy of Sciences, Guiyang 550081, China; University of Chinese Academy of Sciences, Beijing 100049, China*

Sae Yun Kwon − *Division of Environmental Science and Engineering, Pohang University of Science and Technology, Pohang 37673, Republic of Korea;* orcid.org/0000-0001-8665-0327

Ruolan Li − *State Key Laboratory of Environmental Geochemistry, Institute of Geochemistry, Chinese Academy of Sciences, Guiyang 550081, China; University of Chinese Academy of Sciences, Beijing 100049, China*

Chuyan Lai − *State Key Laboratory of Environmental Geochemistry, Institute of Geochemistry, Chinese Academy of Sciences, Guiyang 550081, China; University of Chinese Academy of Sciences, Beijing 100049, China*

Martin Tsz-Ki Tsui − *School of Life Sciences, The Chinese University of Hong Kong, Hong Kong SAR, China;* orcid.org/0000-0003-2002-1530

David Point − *Observatory Midi-Pyrénées, Geosciences Environment Toulouse Laboratory, Research Institute for the Development (IRD), University of Toulouse and CNRS, Toulouse 31400, France*

Jinling Liu − *Hubei Key Laboratory of Critical Zone Evolution, School of Earth Sciences, China University of Geosciences, Wuhan 430074, China;* orcid.org/0000-0002-9989-6550

Yanxu Zhang − *Department of Earth and Environmental Sciences, Tulane University, New Orleans, Louisiana 70118, United States*

Huan Zhong − *School of the Environment, Nanjing University, State Key Laboratory of Pollution Control and Resource Reuse, Nanjing 210023, China;* orcid.org/0000-0002-5100-9465

Runsheng Yin − *State Key Laboratory of Ore Deposit Geochemistry, Institute of Geochemistry, Chinese Academy of Sciences, Guiyang 550081, China;* orcid.org/0000-0002-8072-0774

Zhengcheng Song − *School of Atmospheric Sciences, Nanjing University, Nanjing 210023, China;* orcid.org/0009-0001-4298-8243

Tian Lin − *College of Oceanography and Ecological Science, Shanghai Ocean University, Shanghai 201306, China*

Jingqian Xie − *College of Oceanography and Ecological Science, Shanghai Ocean University, Shanghai 201306, China*

Li Zhang − *Key Laboratory of Tropical Marine Bio-resources and Ecology, Guangdong Provincial Key Laboratory of Applied Marine Biology, South China Sea Institute of Oceanology, Chinese Academy of Sciences, Guangzhou 510301, China;* orcid.org/0000-0001-5705-6548

Xianzhi Lin − *Key Laboratory of Tropical Marine Bio-resources and Ecology, Guangdong Provincial Key Laboratory of Applied Marine Biology, South China Sea Institute of Oceanology, Chinese Academy of Sciences, Guangzhou 510301, China*

Leiming Zhang − *Air Quality Research Division, Science and Technology Branch, Environment and Climate Change Canada, Toronto, Ontario M3H 5T4, Canada*

Xinbin Feng − *State Key Laboratory of Environmental Geochemistry, Institute of Geochemistry, Chinese Academy of Sciences, Guiyang 550081, China; University of Chinese Academy of Sciences, Beijing 100049, China*

Complete contact information is available at: https://pubs.acs.org/10.1021/acs.est.5c12329

Notes

The authors declare no competing financial interest.

■ ACKNOWLEDGMENTS

This work was supported by the Youth Innovation Promotion Association of the Chinese Academy of Sciences (Y2021106), the CAS Interdisciplinary Innovation Team (JCTD-2020-20), the National Natural Science Foundation of China (41573132), and the Key Research Program of Frontier Sciences, Chinese Academy of Sciences (QYZDJ-SSW-DQC005-03).

■ REFERENCES

(1) Krabbenhoft, D. P.; Sunderland, E. M. Global change and mercury. *Science* **2013**, *341*, 1457−1458.

(2) Sunderland, E. M.; Li, M.; Bullard, K. Decadal changes in the edible supply of seafood and methylmercury exposure in the United States. *Environ. Health Perspect.* **2018**, *126*, No. 071006.

(3) Axelrad, D. A.; Bellinger, D. C.; Ryan, L. M.; Woodruff, T. J. Dose−Response relationship of prenatal mercury exposure and IQ: An integrative analysis of epidemiologic data. *Environ. Health Perspect.* **2007**, *115*, 609−615.

(4) Zhang, Y.; Song, Z.; Huang, S.; Zhang, P.; Peng, Y.; Wu, P.; Gu, J.; Dutkiewicz, S.; Zhang, H.; Wu, S.; Wang, F.; Chen, L.; Wang, S.; Li, P. Global health effects of future atmospheric mercury emissions. *Nat. Commun.* **2021**, *12*, No. 3035.

(5) Food and Agriculture Organization of the United Nations (FAO). *The State of World Fisheries and Aquaculture*; FAO: Rome, Italy, 2022.

(6) United Nations Environment Programme (UNEP). *Minamata Convention on Mercury: Text and Annexes*; UNEP: Geneva, Switzerland, 2021.

(7) Wu, P.; Zhang, Y. Toward a Global Model of Methylmercury Biomagnification in marine food webs: trophic dynamics and implications for human exposure. *Environ. Sci. Technol.* **2023**, *57* (16), 6563−6572.

(8) Gehrke, G. E.; Blum, J. D.; Slotton, D. G.; Greenfield, B. K. Mercury isotopes link mercury in San Francisco Bay forage fish to surface sediments. *Environ. Sci. Technol.* **2011**, *45*, 1264−1270.

(9) Blum, J. D.; Popp, B. N.; Drazen, J. C.; Choy, C. A.; Johnson, M. W. Methylmercury production below the mixed layer in the North Pacific Ocean. *Nat. Geosci.* **2013**, *6*, 879−884.

(10) Lavoie, R. A.; Jardine, T. D.; Chumchal, M. M.; Kidd, K. A.; Campbell, L. M. Biomagnification of mercury in aquatic food webs: A worldwide meta-analysis. *Environ. Sci. Technol.* **2013**, *47*, 13385−13394.

(11) Schartup, A. T.; Qureshi, A.; Dassuncao, C.; Thackray, C. P.; Harding, G.; Sunderland, E. M. A model for methylmercury uptake and trophic transfer by marine plankton. *Environ. Sci. Technol.* **2018**, *52*, 654−662.

(12) Chen, C.; Amirbahman, A.; Fisher, N.; Harding, G.; Lamborg, C.; Nacci, D.; Taylor, D. Methylmercury in marine ecosystems: Spatial patterns and processes of production, bioaccumulation, and biomagnification. *EcoHealth* **2008**, *5*, 399−408.

(13) Mason, R. P.; Choi, A. L.; Fitzgerald, W. F.; Hammerschmidt, C. R.; Lamborg, C. H.; Soerensen, A. L.; Sunderland, E. M. Mercury biogeochemical cycling in the ocean and policy implications. *Environ. Res.* **2012**, *119*, 101−117.

(14) Hammerschmidt, C. R.; Fitzgerald, W. F. Sediment−water exchange of methylmercury determined from shipboard benthic flux chambers. *Mar. Chem.* **2008**, *109*, 86−97.

(15) Seelen, E. A.; Chen, C. Y.; Balcom, P. H.; Buckman, K. L.; Taylor, V. F.; Mason, R. P. Historic contamination alters mercury sources and cycling in temperate estuaries relative to uncontaminated sites. *Water Res.* **2021**, *190*, No. 116684.

(16) Balcom, P. H.; Schartup, A. T.; Mason, R. P.; Chen, C. Y. Sources of water column methylmercury across multiple estuaries in the Northeast U.S. *Mar. Chem.* **2015**, *177*, 721−730.

(17) Mason, R. P.; Buckman, K. L.; Seelen, E. A.; Taylor, V. F.; Chen, C. Y. An examination of the factors influencing the bioaccumulation of methylmercury at the base of the estuarine food web. *Sci. Total Environ.* **2023**, *886*, No. 163996.

(18) Walters, D. M.; Cross, W. F.; Kennedy, T. A.; Baxter, C. V.; Hall, R. O., Jr.; Rosi, E. J. Food web controls on mercury fluxes and fate in the Colorado River, Grand Canyon. *Sci. Adv.* **2020**, *6*, No. eaaz4880.

(19) Motta, L. C.; Blum, J. D.; Popp, B. N.; Umhau, B. P.; Benitez-Nelson, C. R.; Close, H. G.; Washburn, S. J.; Drazen, J. C. Mercury isotopic evidence for the importance of particles as a source of mercury to marine organisms. *Proc. Natl. Acad. Sci. U.S.A.* **2022**, *119*, No. e2208183119.

(20) Yin, R.; Feng, X.; Chen, B.; Zhang, J.; Wang, W.; Li, X. Identifying the sources and processes of mercury in subtropical estuarine and ocean sediments using Hg isotopic composition. *Environ. Sci. Technol.* **2015**, *49*, 1347−1355.

(21) Yang, S.; Li, P.; Sun, K.; Wei, N.; Liu, J.; Feng, X. Mercury isotope compositions in seawater and marine fish revealed the sources and processes of mercury in the food web within differing marine compartments. *Water Res.* **2023**, *241*, No. 120150.

(22) Meng, M.; Sun, R.; Liu, H.; Yu, B.; Yin, Y.; Hu, L.; Chen, J.; Shi, J.; Jiang, G. Mercury isotope variations within the marine food web of Chinese Bohai Sea: Implications for mercury sources and biogeochemical cycling. *J. Hazard. Mater.* **2020**, *384*, No. 121379.

(23) Jiskra, M.; Heimbürger-Boavida, L.-E.; Desgranges, M.-M.; Petrova, M. V.; Dufour, A.; Ferreira-Araujo, B.; Masbou, J.; Chmeleff, J.; Thyssen, M.; Point, D.; Sonke, J. E. Mercury stable isotopes constrain atmospheric sources to the ocean. *Nature* **2021**, *597*, 678−682.

(24) Kwon, S. Y.; Blum, J. D.; Yin, R.; Tsui, M. T.-K.; Yang, Y. H.; Choi, J. W. Mercury stable isotopes for monitoring the effectiveness of the Minamata Convention on Mercury. *Earth-Sci. Rev.* **2020**, *203*, No. 103111.

(25) Kwon, S. Y.; Blum, J. D.; Carvan, M. J.; Basu, N.; Head, J. A.; Head, J. A.; Madenjian, C. P.; Madenjian, C. P.; David, S. R. Absence of fractionation of mercury isotopes during trophic transfer of methylmercury to freshwater fish in captivity. *Environ. Sci. Technol.* **2012**, *46*, 7527−7534.

(26) Li, M. L.; Kwon, S. Y.; Poulin, B. A.; Tsui, M. T. K.; Motta, L. C.; Cho, M. Internal dynamics and metabolism of mercury in biota: A review of insights from mercury stable isotopes. *Environ. Sci. Technol.* **2022**, *56*, 9182−9195.

(27) Kwon, S. Y.; Blum, J. D.; Chen, C. Y.; Meattey, D. E.; Mason, R. P. Mercury isotope study of sources and exposure pathways of

methylmercury in estuarine food webs in the northeastern U.S. *Environ. Sci. Technol.* **2014**, *48*, 10089−10097.
(28) Li, M.; Schartup, A. T.; Valberg, A. P.; Ewald, J. D.; Krabbenhoft, D. P.; Yin, R.; Balcom, P. H.; Sunderland, E. M. Environmental Origins of Methylmercury accumulated in subarctic estuarine fish indicated by mercury stable isotopes. *Environ. Sci. Technol.* **2016**, *50*, 11559−11568.
(29) Lim, S. H.; Kim, Y.; Motta, L. C.; Yang, E. J.; Rhee, T. S.; Hong, J. K.; Han, S.; Kwon, S. Y. Near surface oxidation of elemental mercury leads to mercury exposure in the Arctic Ocean biota. *Nat. Commun.* **2024**, *15*, No. 7598.
(30) Senn, D. B.; Chesney, E. J.; Blum, J. D.; Bank, M. S.; Maage, A.; Shine, J. P. Stable isotope (N, C, Hg) study of methylmercury sources and trophic transfer in the northern Gulf of Mexico. *Environ. Sci. Technol.* **2010**, *44*, 1630−1637.
(31) Tsui, M. T. K.; Blum, J. D.; Kwon, S. Y.; Finlay, J. C.; Balogh, S. J.; Nollet, Y. H. Sources and transfers of methylmercury in adjacent river and forest food webs. *Environ. Sci. Technol.* **2012**, *46*, 10957−10964.
(32) Masbou, J.; Point, D.; Sonke, J. E. Application of a selective extraction method for methylmercury compound specific stable isotope analysis (MeHg-CSIA) in biological materials. *J. Anal. At. Spectrom.* **2013**, *28* (10), 1620−1628.
(33) Yang, S.; Wang, B.; Qin, C.; Yin, R.; Li, R.; Liu, J.; Liu, J.; Point, D.; Point, D.; Maurice, L.; Maurice, L.; Sonke, J. E.; Sonke, J. E.; Zhang, L.; Zhang, L.; Feng, X. Compound-specific stable isotope analysis provides new insights for tracking human monomethylmercury exposure sources. *Environ. Sci. Technol.* **2021**, *55*, 12493−12503.
(34) Hofstetter, T. B.; Bakkour, R.; Buchner, D.; Eisenmann, H.; Fischer, A.; Gehre, M.; Haderlein, S. B.; Höhener, P.; Hunkeler, D.; Imfeld, G.; Jochmann, M. A.; Kümmel, S.; Martin, P. R.; Pati, S. G.; Schmidt, T. C.; Vogt, C.; Elsner, M. Perspectives of compound-specific isotope analysis of organic contaminants for assessing environmental fate and managing chemical pollution. *Nat. Water* **2024**, *2*, 14−30.
(35) Fu, X.; Feng, X.; Zhang, G.; Xu, W.; Li, X.; Yao, H.; Liang, P.; Li, J.; Sommar, J.; Yin, R.; Liu, N. Mercury in the marine boundary layer and seawater of the South China Sea: Concentrations, sea/air flux, and implication for land outflow. *J. Geophys. Res.* **2010**, *115*, No. D06303.
(36) Li, K.; Lin, C.-J.; Yuan, W.; Sun, G.; Fu, X.; Feng, X. An improved method for recovering and preconcentrating mercury in natural water samples for stable isotope analysis. *J. Anal. At. Spectrom.* **2019**, *34*, 2303−2313.
(37) Yan, Y.; Yi, M.; Feng, B. *Atlas Guide to Economic Fishes of South China Sea*; Science Press: Beijing, 2021.
(38) Zhuang, P.; Zhang, Y.; Zhao, H. *Fishes of Coastal China Seas*; China Agriculture Press: Beijing, 2021; Vol. *III*.
(39) U.S. Environmental Protection Agency (USEPA). *Mercury in Water by Oxidation, Purge and Trap, and Cold Vapor Atomic Fluorescence Spectrometry; Method 1631*; Revision E; U.S. Environmental Protection Agency: Washington, DC, 2002.
(40) Meng, M.; Sun, R.; Liu, H.; Yu, B.; Yin, Y.; Hu, L.; Shi, J.; Jiang, G. An integrated model for input and migration of mercury in Chinese coastal sediments. *Environ. Sci. Technol.* **2019**, *53*, 2460−2471.
(41) Yin, R.; Feng, X.; Zhang, J.; Pan, K.; Wang, W.; Li, X. Using Mercury isotopes to understand the bioaccumulation of Hg in the subtropical Pearl River Estuary, South China. *Chemosphere* **2016**, *147*, 173−179.
(42) Xu, X. Y.; Zhang, Q. G.; Wang, W. X. Linking mercury, carbon, and nitrogen stable isotopes in Tibetan biota: Implications for using mercury stable isotopes as source tracers. *Sci. Rep.* **2016**, *6*, No. 25394.
(43) Zhang, H.; Wang, W.; Lin, C.; Feng, X.; Shi, J.; Jiang, G.; Larssen, T. Decreasing mercury levels in consumer fish over the three decades of increasing mercury emissions in China. *Eco-Environ. Health* **2022**, *1*, 46−52.
(44) Blum, J. D.; Sherman, L. S.; Johnson, M. W. Mercury isotopes in earth and environmental sciences. *Annu. Rev. Earth Planet. Sci.* **2014**, *42*, 249−269.
(45) Tsui, M. T. K.; Uzun, H.; Ruecker, A.; Majidzadeh, H.; Ulus, Y.; Zhang, H.; Bao, S.; Blum, J. D.; Karanfil, T.; Chow, A. Concentration and isotopic composition of mercury in a blackwater river affected by extreme flooding events. *Limnol. Oceanogr.* **2020**, *65*, 2158−2169.
(46) Lee, C. S.; Fisher, N. S. Methylmercury uptake by diverse marine phytoplankton. *Limnol. Oceanogr.* **2016**, *61*, 1626−1639.
(47) Liang, X.; Zhong, H.; Johs, A.; Lei, P.; Zhang, J.; Taş, N.; Zhang, L.; Zhao, L.; Zhu, N.; Yin, X.; Wang, L.; Zeng, E. Y.; Gao, Y.; Zhao, J.; Pelletier, D. A.; Pierce, E. M.; Gu, B. Light-independent phytoplankton degradation and detoxification of methylmercury in water. *Nat. Water* **2023**, *1*, 705−715.
(48) Motta, L. C.; Blum, J. D.; Johnson, M. W.; Umhau, B. P.; Popp, B. N.; Washburn, S. J.; Drazen, J. C.; Benitez-Nelson, C. R.; Hannides, C. C. S.; Close, H. G.; Lamborg, C. H. Mercury cycling in the North Pacific subtropical gyre as revealed by mercury stable isotope ratios. *Glob. Biogeochem. Cycles* **2019**, *33*, 777−794.
(49) Bergquist, B. A.; Blum, J. D. Mass-dependent and independent fractionation of Hg isotopes by photoreduction in aquatic systems. *Science* **2007**, *318*, 417−420.
(50) Sun, R.; Yuan, J.; Sonke, J. E.; Zhang, Y.; Zhang, T.; Zheng, W.; Chen, S.; Meng, M.; Chen, J.; Liu, Y.; Peng, X.; Liu, C. Methylmercury produced in upper oceans accumulates in deep Mariana Trench fauna. *Nat. Commun.* **2020**, *11*, No. 3389.
(51) Ma, X.; Chen, G. Marine heatwaves are shaping the vertical structure of phytoplankton in the global ocean. *Commun. Earth Environ.* **2025**, *6*, No. 715.
(52) Tsz-Ki Tsui, M.; Kwon, S. Y.; Li, M. L.; Bishop, K. Revisiting the relationship between mercury emission and bioaccumulation. *Eco-Environ. Health* **2023**, *2*, 1−2.
(53) Chen, C. F.; Ju, Y. R.; Chen, C. W.; Dong, C. D. The distribution of methylmercury in estuary and harbor sediments. *Sci. Total Environ.* **2019**, *691*, 55−63.
(54) Wang, J.; Dai, J.; Chen, G.; Jiang, F. Role of sulfur biogeochemical cycle in mercury methylation in estuarine sediments: A review. *J. Hazard. Mater.* **2022**, *423*, No. 126964.
(55) Shi, J.; Wang, T.; Li, C.; Zhao, J.; Kang, Z.; Song, X.; Liu, Y. Food web structure and trophic diversity for the fishes of four islands in the Pearl River Estuary, China. *Ecol. Indic.* **2024**, *160*, No. 111916.
(56) Zhou, L.; Yang, X.; Li, K.; Xiang, C.; Wu, Y.; Huang, X.; Huang, L.; Tan, Y. Regime shift in a coastal pelagic ecosystem with increasing human-induced nutrient inputs over decades. *Water Res.* **2024**, *263*, No. 122147.
(57) Nam, N. T.; Miller, T. W.; Huan, N. X.; Tang, V. T.; Omori, K. Integrating community structure and stable isotope analysis to assess a heavily exploited coastal marine ecosystem off central Vietnam. *Fish. Res.* **2011**, *110*, 268−276.
(58) Médieu, A.; Spitz, J.; Point, D.; Sonke, J. E.; Loutrage, L.; Laffont, L.; Chouvelon, T. Mercury stable isotopes reveal the vertical distribution and trophic ecology of deep-pelagic organisms over the North-East Atlantic Ocean continental slope. *Environ. Sci. Technol.* **2024**, *58*, 18733−18743.
(59) China Fishery Press. *China Fishery Statistical Yearbook (2011−2020)*; China Fishery Press: Beijing, 2020.
(60) Schartup, A. T.; Thackray, C. P.; Qureshi, A.; Dassuncao, C.; Gillespie, K.; Hanke, A.; Sunderland, E. M. Climate change and overfishing increase neurotoxicant in marine predators. *Nature* **2019**, *572*, 648−650.
(61) Wu, P.; Zakem, E. J.; Dutkiewicz, S.; Zhang, Y. Biomagnification of methylmercury in a marine plankton ecosystem. *Environ. Sci. Technol.* **2020**, *54*, 5446−5455.
(62) Zhang, Y.; Soerensen, A. L.; Schartup, A. T.; Sunderland, E. M. A global model for methylmercury formation and uptake at the base of marine food webs. *Glob. Biogeochem. Cycles* **2020**, *34*, No. e2019GB006348.

https://doi.org/10.1021/acs.est.5c12329
Environ. Sci. Technol. 2026, 60, 5711−5723

(63) Warren, G. J.; Lesht, B. M.; Barbiero, R. P. Estimation of the width of the nearshore zone in Lake Michigan using eleven years of MODIS satellite imagery. *J. Great Lakes Res.* **2018**, *44*, 563−572.
(64) Pauly, D.; Zeller, D. Catch reconstructions reveal that global marine fisheries catches are higher than reported and declining. *Nat. Commun.* **2016**, *7*, No. 10244.
(65) Allison, E. H.; Perry, A. L.; Badjeck, M.-C.; Adger, W. N.; Brown, K.; Conway, D.; Halls, A. S.; Pilling, G. M.; Reynolds, J. D.; Andrew, N. L.; Dulvy, N. K. Vulnerability of national economies to the impacts of climate change on fisheries. *Fish Fish.* **2009**, *10*, 173−196.
(66) Ci, Z.; Shen, W.; Chen, B.; Li, Y.; Yin, Y.; Zhang, X.; Cai, Y. Potential increase of neurotoxic mercury risk in global blue carbon nature-based solutions. *Nat. Sustainable* **2024**, *7*, 1592−1595.

https://doi.org/10.1021/acs.est.5c12329
Environ. Sci. Technol. 2026, 60, 5711−5723